

Gravity Current around Circular Cylinder

By

Leong Chi Seng



Master of Science in Civil Engineering

2009



**Faculty of Science and Technology
University of Macau**

GRAVITY CURRENT AROUND CIRCULAR CYLINDER

By

Leong Chi Seng

A thesis submitted in partial fulfillment of the
requirements for the degree of

Master of Science in Civil Engineering

Faculty of Science and Technology
University of Macau

2009



Approved by _____

Supervisor

Date _____

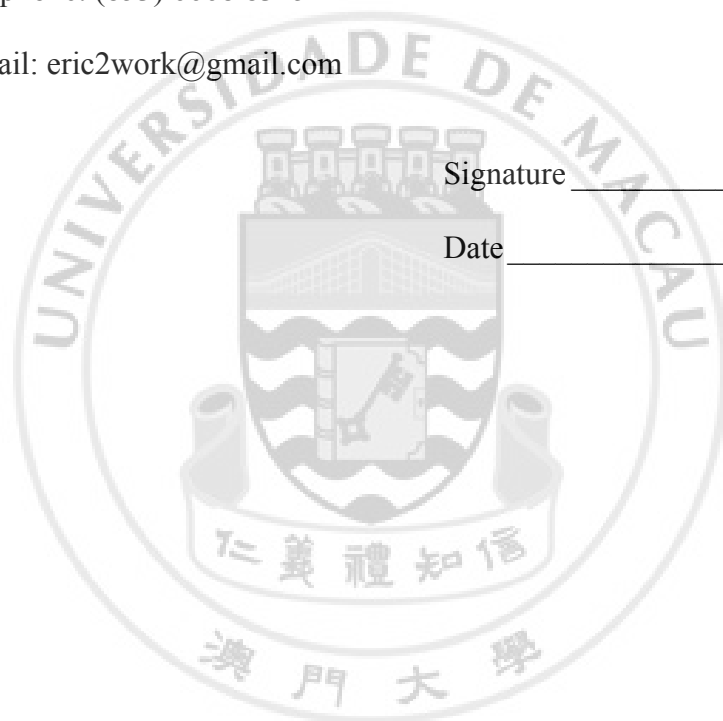
In presenting this thesis in partial fulfillment of the requirements for a Master's degree at the University of Macau, I agree that the Library and the Faculty of Science and Technology shall make its copies freely available for inspection. However, reproduction of this thesis for any purposes or by any means shall not be allowed without my written permission. Authorization is sought by contacting the author at

Address: Rua da Perola Oriental No.97, 27 andar IC

Telephone: (853) 6668 8325

Fax:

E-mail: eric2work@gmail.com



Signature _____

Date _____

University of Macau

Abstract

Gravity Current around Circular Cylinder
By Leong Chi Seng

Thesis Supervisor: Prof. K. M. Mok
Department of Civil and Environmental Engineering

The present study is to exam the interaction of a fully developed gravity current with a circular cylinder. A series of experiment was performed in a water tank of 16.62 m long, 0.61m wide and 0.45 m deep. The lock exchange scheme was used for generation of the gravity current. Specific gravity of the saline water used for current generation in the experiments was controlled in the range of 1.0035 to 1.0040. Motions of the gravity current interacting with a 14 cm diameter circular cylinder situating at 5.05 m downstream were recorded with a 3CCD digital camera with the Laser Induced Fluorescence (LIF) technique. Quantitative and qualitative results of these experiments are reported.

In general, when the current met the cylinder, two main processes were observed. Part of it split and went around the cylinder while part would run up the cylinder front. The split current merged back together at the downstream end of the cylinder and appeared as a fully developed one at about 1.7 to 1.9D (D = diameter of cylinder) downstream of it.

From the present observations, the run up process of the current on the cylinder front could be divided into three stages; they are impact stage, transition stage, and steady stage. The maximum run up heights of the impact stage and transition stage were 55-65% and 73 % of the total water depth, respectively. Variation of the observed maximum run up height at the impact stage appeared to depend on the Froude number of the incoming current. At the same time, the maximum run up height in the transition stage could be controlled by the flow circulation induced by the reverse

fresh water flow around the cylinder and above the saline water. The steady stage of the run up process on the cylinder began when the first reflected jump in the upstream end of the cylinder occurred. It was found that the subsequent reflected disturbances had a cyclic characteristic influenced by the vortex shedding process generated from the reversed fresh water flow around the cylinder in the upper fluid layer.



TABLE OF CONTENTS

LIST OF FIGURES	iii
LIST OF TABLES	ix
CHAPTER 1: Introduction	1
CHAPTER 2: Background of Gravity Current.....	5
2.1 Gravity currents on horizontal surface.....	5
2.2 Gravity currents encounter obstacles.....	9
2.2.1 Analysis with passiver upper layer	9
2.2.2 Analysis with active upper layer.....	12
2.3 Wake behind circular cylinder.....	16
CHAPTER 3: Experiments.....	18
3.1 Experimental set up.....	18
3.2 Experimental Procedure.....	20
3.3 Post-processing.....	23
CHAPTER 4: Results and Discussion.....	25
4.1 Results of transverse viewing plane.....	26
4.1.1 At 0.5 cm upstream of cylinder ($X = -0.5$ cm)	26
4.1.2 At 11.5 cm upstream of cylinder ($X = -11.5$ cm)	31
4.1.3 At 0.5 cm downstream of cylinder ($X = 14.5$ cm).....	36
4.1.4 At 11.5 cm downstream of cylinder ($X = 25.5$ cm).....	40
4.1.5 Center of cylinder ($X = 7$ cm).....	43
4.2 Results of horizontal viewing plane.....	47
4.2.1 At 1.5 cm above the tank bottom ($Z = 1.5$ cm).....	47
4.2.2 At 7 cm above the tank bottom ($Z = 7$ cm).....	49
4.2.3 At 8 cm above the tank bottom ($Z = 8$ cm).....	51
4.3 Results of longitudinal viewing plane.....	53
4.3.1 At 0.5 cm from the tangent edge of cylinder ($Y = -7.5$ cm)	53
4.3.2 At 11.5 cm from the tangent edge of cylinder($Y = -18.5$ cm)	57
4.3.3 Along the centerline of tank at downstream of cylinder.....	62
4.3.4 Along the centerline of tank at upstream of cylinder.....	65

4.4 Discussion of results	94
4.4.1 Before the current encounter the cylinder.....	94
4.4.2 After the current encounter the cylinder	95
CHAPTER 5: Conclusion	101
BIBLIOGRAPHY	102
APPENDIX A: Two dimensional linear interpolation function	104
APPENDIX B: Calculation of the power spectrum.....	106



LIST OF FIGURES

<i>Number</i>	<i>Page</i>
Figure 1.1: Diagram of gravity current propagating along a plane. Area with dotted line is the region of “head”	2
Figure 2.1: Analytic scheme of steady flow past a cavity by Benjamin (1968).	7
Figure 2.2: Shin et al. (2004) suggested schematic of partial depth lock release analysis (a) before release & (b) after release. U_r is the velocity of backward disturbance of denser fluid and u_1 is velocity of lighter fluid.	8
Figure 2.3: Schematic illustration with shallow two-layer flow over a wall, showing the hydraulic jump propagating upstream Rottman et al. (1985).	10
Figure 2.4: Solutions of steady shallow-water equation for the depth of the fluid behind the hydraulic jump as a function of the wall height h_w	12
Figure 2.5: Diagram in active upper layer analysis, the flow after the gravity current meet the obstacle has been partially reflected with rigid lid (Lane-Serff et al. 1995)	13
Figure 2.6: The wake pattern in different value of Reynolds number (Williamson 1996).	16
Figure 3.1: Schematic of experiment set up.	18
Figure 3.2: (a) Stainless steel gate and pneumatic cylinder; (b) temper glass sidewall of the hydraulic tank	19
Figure 3.3: Temper glass of tank floor observation area; (b) circular cylinder of 14cm in diameter.	19
Figure 3.4: (a) Argon-ion laser (Coherent Innova 70-4); (b) scanner drive (General Scanning Ax-200) and function generator (Tektroniz CFG 280).	20

Figure 3.5:	Showing observation of flow-field planes parallel to the flow direction (1) center and upstream of cylinder (2) tangent to the cylinder (3) 11.5 cm from the cylinder (4) center and downstream of cylinder.....	21
Figure 3.6:	Showing observation of flow-field planes perpendicular to the flow direction (5) tangent to the cylinder in downstream, (6) 11.5 cm apart from the cylinder in downstream, (7) center of cylinder, (8) tangent to the cylinder in upstream, (9) 11.5 cm apart from the cylinder in upstream.	21
Figure 3.7:	Showing observation of the horizontal planes (10) 1.5 cm apart from the bottom; (11) 7 cm from the bottom; (12) 8 cm from the bottom.....	22
Figure 3.8:	Calibration board with reference grid (a) center of cylinder (transverse direction); (b) upstream of cylinder (longitudinal direction)	24
Figure 3.9:	Coordinate of calculation for calibration.....	24
Figure 4.1:	The gravity current front of experimental run no. 10 flowing through the transverse-vertical plane located at 0.5 cm upstream from cylinder; (a) 114.76 sec.; (b) 115.36 sec.; (c) 116.76 sec.; (d) 122.08 sec.; (e) 125.08 sec.; (f) 126.08 sec.; (g) 126.64 sec.; (h) 131.12 sec.; (i) 134.88 sec.; (j) 170.92 sec.; after the gate opening.....	27
Figure 4.2:	Measurement results of experiment no.10 (a) time history of depth at center; (b) time history of depth at center in impact & transition stage; (c) time history of depth at center in steady stage; (d) running up velocity with time during impact stage upward motion.....	30
Figure 4.3:	The gravity current front in experimental run no. 11 flowing through the vertical plane located at 11.5 cm upstream from cylinder; (a) 94.12 sec.; (b) 95.32 sec.; (c) 96.32 sec.; (d) 99.32 sec.; (e) 100.84 sec.; (f) 110.32 sec.; (g) 113.32 sec.; (h) 116.32 sec.; after the gate opening.....	33

Figure 4.4:	The gravity current front in experimental run no. 12 flowing through the vertical plane located at 11.5 cm upstream from cylinder; (a) 100.6 sec.; (b) 101.4 sec.; (c) 103.8 sec.; (d) 109.8 sec.; (e) 112.8 sec.; (f) 116.6 sec.; (g) 120.6 sec.; (h) 125.28 sec.; after the gate opening	35
Figure 4.5:	The gravity current front in experimental run no. 6 flowing through the vertical plane located at 0.5 cm downstream from cylinder; (a) 113.88 sec.; (b)114.88 sec.; (c) 116.16 sec.; (d) 119.76 sec.; (e) 122.08 sec.; (f) 128.08sec.; after the gate opening.....	37
Figure 4.6:	The gravity current front in experimental run no. 7 flowing through the vertical plane located at 0.5 cm downstream from cylinder; (a) 120.84 sec.; (b) 121.64 sec.; (c) 123.32 sec.; (d) 126.76 sec.; (e) 129.24 sec.; (f) 144.12 sec.; after the gate opening.....	39
Figure 4.7:	The gravity current front in experimental run no. 8 flowing through the vertical plane located at 11.5 cm downstream from cylinder; (a) 106 sec; (b) 107 sec.; (c) 107.56 sec.; (d) 107.8 sec.; (e) 108.52 sec.; (f) 109.4 sec.; (g) 111.96 sec.; (h) 113sec.; (i) 114.28 sec.; (j) 115.08 sec.; (k) 116.56 sec.; (l) 125.88 sec.; after the gate opening.....	41
Figure 4.8:	Time history of depth at center during flowing through the vertical plane 11.5cm downstream of cylinder in experimental run no. 8.....	43
Figure 4.9:	The gravity current front in experimental run no. 9 flowing through the transverse plane located at X = 7 cm; (a) 104.12 sec.; (b) 105.12 sec.; (c) 105.32 sec.; (d) 109.52 sec.; (e) 113.12 sec.; (f) 115.04 sec.; (g) 116.56 sec.; (h) 125.36 sec. after the gate opening.....	44
Figure 4.10:	Time history of the depth at Y = -7.5cm obtained from experiment no.9.....	47

Figure 4.11: The gravity current front in experimental run no. 13 flowing through the horizontal viewing plane located at 1.5 cm above the bottom of tank; (a)92.8 sec.; (b) 95.92 sec.; (c) 96.92 sec.; (d) 99.32 sec.; (e) 100.48 sec.; (f) 103.2 sec.; after the gate opening.	48
Figure 4.12: The gravity current front in experimental run no. 14 flowing through the horizontal viewing plane located at 7 cm above the bottom of tank; (a)101.92 sec.; (b) 103.52 sec.; (c) 104.8 sec.; (d) 105.4 sec.; (e) 106.12 sec.; (f) 106.24 sec.; (g) 106.92 sec.; (h) 107.72 sec.; after the gate opening.	50
Figure 4.13: The gravity current front in experimental run no. 15 flowing through the horizontal viewing plane located at 8 cm above the bottom of tank; (a)149.84 sec.; (b) 151.12 sec.; (c) 151.72 sec.; (d) 152.92 sec.; (e) 153.92 sec.; (f) 155.04 sec.; after the gate opening.	52
Figure 4.14: The gravity current front propagating in a longitudinal vertical plane tangent to cylinder ($Y = -7.5$ cm) in experimental run no. 2, (a)103.88 sec.; (b) 105.96 sec.; (c) 106.4 sec.; (d) 106.8 sec.; (e) 107.52 sec.; (f) 108.2 sec.; (g) 109.08 sec.; (h) 111.08 sec.; (i) 112.92 sec.; (j) 113.08 sec.; (k) 122.08 sec.; (l) 127 sec.; after the gate opening.	55
Figure 4.15: Density current propagation along vertical plane 0.5 cm distant from the tangent line of circular cylinder ($Y = -7.5$ cm) in experiment no. 2 ; (a) time history of location of front in X direction; (b) advancing velocity of front with the time.	57
Figure 4.16: The gravity current front propagating in a longitudinal vertical plane 11.5 mm from the edge of circular cylinder in experimental run no. 3, (a)130.12 sec.; (b) 130.6 sec.; (c) 131.2 sec.; (d) 131.92 sec.; (e) 132.32 sec.; (f) 134.2 sec.; (g) 134.44 sec.; (h) 136.12 sec.; (i) 138.04 sec.; (j) 138.52 sec.; (k) 148.6 sec.; (l) 153.64 sec.; after the gate opening.	59

Figure 4.17: Density current propagation along vertical plane 11.5 cm distant from the tangent line of circular cylinder in experiment no.3; (a) time history of location of front in X direction; (b) advancing velocity of front with time.	61
Figure 4.18: The gravity current front propagating along a longitudinal vertical plane downstream of cylinder and center of the tank in experiment no. 1, (a)126.16 sec.; (b) 126.44 sec.; (c) 127.8 sec.; (d) 128.4 sec.; (e) 130.2 sec.; (f) 130.68 sec.; (g) 131.8 sec.; (h) 133.2 sec.; (i) 133.6 sec.; (j) 137.8 sec.; after the gate opening.	63
Figure 4.19: Measurement results of experiment no.1; (a) time history of the location of front nose; (b) variation of the advancing velocity of front respect to the nose location.	65
Figure 4.20: The gravity current front propagating along center line upstream of cylinder in experimental run no. 4, (a) 96.24 sec.; (b) 96.48 sec.; (c) 96.68 sec.; (d) 97 sec.; (e) 97.76 sec.; (f) 98.04sec.; (g) 98.76 sec.; (h) 99.56sec.; after the gate opening.	66
Figure 4.21: Impact stage running up of gravity current along the edge of cylinder in experimental run no. 4, (a) 101.04sec.; (b) 102 sec.; (c) 103.52 sec.; (d) 104.26 sec.; (e) 104.42 sec.; (f) 106.64 sec.; (g) 107.36 sec.; (h) 107.64 sec.; after the gate opening.	68
Figure 4.22: Transition & steady stage of running up process in experimental run no. 4, (a) 109.12 sec.; (b) 110.12 sec.; (c) 110.92 sec.; (d) 111.84 sec.; (e) 112.44 sec.; (f) 113.76 sec.; (g) 115.48 sec.; (h) 117.08 sec.; (i) 119.16 sec.; (j) 121.16 sec.; (k) 133.44 sec.; (l) 165.92 sec; after the gate opening.	70
Figure 4.23: The gravity current front propagating along center line upstream of cylinder in experimental run no. 5, (a) 101.76 sec.; (b) 102.04 sec.; (c) 102.48 sec.; (d) 103.8 sec.; (e) 103.96 sec.; (f) 104.46 sec.; (g) 106.4 sec.; (h) 107.16 sec.; (i) 107.48 sec.; (j) 108.28 sec.; after the gate opening.	73

Figure 4.24:	Impact stage running up of gravity current along the edge of cylinder in experimental run no. 5, (a) 108.4 sec.; (b) 108.72 sec.; (c) 110.72 sec.; (d) 111.32 sec.; (e) 111.96 sec.; (f) 113.48 sec.; after the gate opening.....	75
Figure 4.25:	Transition and steady stage of running up process in experimental run no. 5, (a) 115.8 sec.; (b) 119.32 sec.; (c) 121.56 sec.; (d) 122.36 sec.; (e) 123.56 sec.; (f) 126.68 sec.;(g) 127.08 sec.; (h) 129.16 sec.; after the gate opening	77
Figure 4.26:	Variation of advancing velocity with respect to longitudinal distance apart from circular cylinder; (a1) experimental no. 4; (b1) experimental no.5; Variation of nose height with respect to longitudinal distance apart from circular cylinder (a2) experimental no. 4; (b2) experimental no. 5.....	80
Figure 4.27:	Variation of run up height with time; (a) experimental run no. 4; (b) experimental run no. 5.....	82
Figure 4.28:	Time history of the run up height in impact stage; (a1) experimental run no. 4; (b1) experimental run no. 5; Time history of run up velocity in impact stage; (a2) experimental run no. 4; (b2) experimental run no. 5.....	84
Figure 4.29:	Measurement of interface fluctuation in steady stage.....	86
Figure 4.30a:	Depth of interface in experiment no. 4 (a1) X=-10 cm; (a2) X=-15cm; (a3) X=-20cm; (a4) X=-25cm; (a5) X=-30cm.....	87
Figure 4.30b:	Depth of interface in experiment no.5 (b1) X=-10 cm; (b2) X=-15cm; (b3) X=-20cm; (b4) X=-25cm; (b5) X=-30cm.....	88
Figure 4.31:	Energy spectrum of the interface fluctuation in steady stage; Experiment no.4 (a1) at X=-110 cm; (a2) X=-15 cm; (a3) X=-20 cm; (a4) X=-25 cm; (a5) X=-30 cm; Experiment no.5 (b1) X=-10 cm; (b2) X=-15 cm; (b3) X=-20 cm; (b4) X=-25 cm; (b5)X=- 30 cm.....	91
Figure 4.32:	Height of run up current in steady stage (a) experiment no.4; (b) experiment no.5.....	93
Figure 4.33:	Schematic of generating circulation of fresh water.....	98

LIST OF TABLES

<i>Number</i>	<i>Page</i>
Table 3.1: Information of gravity current experiments at different observing plane.....	22
Table 4.1: Time period for three stages of upward motion along the foremost edge of cylinder ($X=0$).....	83
Table 4.2: Average depth of the interface in experiment no.4 and no.5.....	90
Table 4.3: The frequency of main energy at different location in experimental run no.4 and no.5.....	93
Table 4.4: Comparison of impact stage among the experiment no.4, no.5 and no.10.....	97

